# Substituent Effects on the Spin Equilibrium Observed with Hexadentate Ligands on Iron(II)[1]

**Mitchell A. Hoselton,[2] Lon J. Wilson,[3] and Russell S. Drago*[2]**

*Contribution from the W. A. Noyes Laboratory, University of Illinois, Urbana, Illinois 61801, and the Department of Chemistry, William Marsh Rice University, Houston, Texas 77001.* *Received May 14, 1974*

**Abstract:** A new series of pseudooctahedral Fe(II) complexes derived from the hexadentate ligand tris{4-[(6-*R*)-2-pyridyl]-3-aza-3-butenyl}amine, where R is either H or $CH_3$ (Figure 1), has been synthesized and studied. Magnetic susceptibility and Mössbauer measurements demonstrate that compounds II, III, and IV as their $PF_6^-$ salts undergo a high ↔ low "spin equilibrium" in the solid state. Additionally, Evans' method solution measurements indicate that II and III also exhibit the same phenomenon in solution. Thus, these complexes are among the first Fe(II) chelates to provide evidence for the existence of the spin equilibrium process in solution. An X-ray structural study of compound IV performed by Delker and Stucky indicates that a steric interaction between the methyl groups and adjacent pyridine rings is largely responsible for the observed changes in the magnetic behavior of the series as the number of methyl substituted ligand arms is varied. Furthermore, the variable temperature structural data for IV shows an average decrease of ~0.12 Å in the six Fe–N bond distances in going from the fully high spin state ($\mu_{eff}$ ~ 5.0 BM at 300°K) to a state of intermediate spin ($\mu_{eff}$ ~2.3 BM at 205°K). The results reported here indicate that multidentate ligands can be of general utility in designing new spin equilibrium systems where ligand substituent effects may be employed to "fine-tune" the ligand field strength around the crossover region.

Transition metal complexes exhibiting spin equilibria between two electronic ground states have been recognized and studied for more than 10 years.[4-11] Usually these studies have focused on interpretation of the anomolous magnetic behavior which arises at or near the crossover region where electron spin pairing and ligand field splitting energies become competitive. To date, most studies of this nature have been restricted to the solid state, presumably due to the disappearance of the necessary equilibrium conditions in solution or to compound instability in the solution state. In particular for Fe(II), the only spin equilibrium system to be well characterized in both the solid and solution states is the poly(1-pyrazolyl)borate Fe(II) complex reported by Jesson and coworkers.[4] It would seem desirable to develop and study spin equilibrium processes in the solution state as well as in solids since: (1) reports of such studies in solution have been rare, (2) comparative solution–solid state studies should be mutually complimentary in understanding lattice and solution environment contributions to the overall equilibrium process, and (3) the spin equilibrium dependency of electron transfer reactions in solution is of fundamental importance in modern reaction mechanism theory,[12] as well as being implicated in some metalloprotein electron transfer activity.[13]

As an initial approach toward obtaining solid *vs.* solution state data for spin equilibrium processes, we have synthesized a series of hexadentate ligands designed to support an $^1A_{1g} \leftrightarrow {}^5T_{2g}$ spin equilibrium for Fe(II). Multidentate ligands were thought especially desirable in order to enhance the solution state stability of the complexes by taking advantage of the "chelate effect." This expectation has apparently been realized in the present study. The ligands chosen for investigation are of the strong-field tris($\alpha$-diimine) variety and have been derived from the Schiff base condensation of the tetramine, tris(2-aminoethyl)amine (tren), with the appropriate pyridinecarboxyaldehyde(s) (Figure 1). This particular series of ligands was selected because the structurally related tris(1,10-phenanthroline)iron(II) and tris(2-methyl-1,10-phenanthroline)iron(II) complexes were known to span the entire spin state range for Fe(II), the former being low-spin and the latter high-spin at room temperature.[14] The multidentate ligands of Figure 1, however, offer an added advantage over the trisbidentate variety in that they permit addition of the methyl groups singly, thereby allowing a step-wise "fine-tuning" of the ligand field strength in and around the crossover region. The synthesis and characterization of compounds I and IV in Figure 1 have been previously reported;[15] II and III are new derivatives and their syntheses are reported here for the first time.

The hexadentate nature of the ligands in I and IV have been verified by single-crystal X-ray studies.[16,17] The Fe–N(7) distances are found to be very long at 3.44 and 3.31 Å, respectively, and thus a bonding interaction at this position may be disregarded in a first approximation. In addition to establishing the hexadentate nature of the ligands, the X-ray data in Table I also indicate that the effective molecular geometry of I is best described as a slightly distorted trigonal antiprism (or octahedron). For the idealized geometry, the Fe(II) atom would lie in the center of the coordination polyhedron defined by the upper (three imine N's) and lower (three pyridine N's) triangular faces which would be twisted relative to one another by an angle, $\theta$ = 60°. The actual structure of I approaches the idealized polyhedron with $\theta_{av}$ = 54° and the Fe–N(imine) and Fe–N(pyridine) distances of 1.94 and 1.96 Å being nearly equal. In fact, an octahedral assignment is probably as good an approximation for I as it is for the tris(1,10-phenanthroline)iron(II) complex where $\theta$ is also 54°.[18] For IV, with $\theta_{av}$ = 51° and Fe–N(imine) and Fe–N(pyridine) bond distances of 2.14 and 2.28 Å at room temperature, the coordination polyhedron is somewhat more distorted but still reasonably well approximated by an octahedral model. Based on these X-ray results, the spin equilibria observed for compounds II–IV have been interpreted on a trigonally distorted octahedral model for Fe(II) (see Magnetic Discussion below).

## Experimental Section

**Physical Measurements.** Magnetic susceptibilities of the solid complexes were measured by the Faraday method. Pascal constants were used to correct for ligand diamagnetism. Measurements in acetone and DMSO solutions were evaluated using Evans' method[19] and were corrected for changes in solvent density with temperature.[20] At elevated temperatures, the complexes have a tendency to decompose slowly. In the solution samples, this effect was minimized by using fresh samples at each temperature. In the solids, this was not feasible; however, the weight loss of solid material was never larger than 2% and the largest expected errors are

Table I. Selected Structural Parameters for the Fe(II) Coordination Polyhedra

| Compound ($PF_6^-$ salt) | $T$ (°K) | Fe–N(pyridine)[c] (Å) | Fe–N(imine)[c] (Å) | Fe–N(7) (Å) | Av. $\theta$ angle[d] (deg) |
|---|---|---|---|---|---|
| I[a] | 300 | 1.966 | 1.942 | 3.439 | 54 |
| IV[b] | 300 | 2.282 | 2.143 | 3.314 | 51 |
| | 205 | 2.142 | 2.043 | 3.452 | |

[a] C. Mealli and E. C. Lingafelter, *Chem. Commun.*, 885 (1970); E. C. Lingafelter, private communication. [b] Private communication, G. Delker and G. D. Stucky, School of Chemical Sciences, University of Illinois. [c] Average of the three Fe–N distances. [d] $\theta = 60°$ in $O_h$ symmetry.

restricted to the highest temperatures. Possible complications in the analysis by Evans' method arising from specific solvent–solute interactions have been shown to be negligible for these systems by comparison of the splitting of the resonances due to the solvent with those for an inert reference such as TMS or benzene. In all cases, the magnetic moments calculated for the various resonances were constant within experimental error.

Mössbauer spectra were obtained on an apparatus previously described.[13] Pmr spectra were run at 60 MHz on a Joelco C60-H and at 220 MHz on a Varian HR-220. Uv–visible and ir spectra were run on the Cary 14 and the Perkin-Elmer 457 grating infrared spectrophotometer, respectively. Polarographic measurements were obtained with a Princeton Applied Research Model 174 polarograph at a rotating platinum electrode. Data were obtained in acetone using 0.1 *M* tetraethylammonium perchlorate as the supporting electrolyte. The $E_{1/2}$ potentials are referenced to the saturated calomel electrode (sce).

**Materials and Preparations.** All reagents used were of the highest available purity and, unless otherwise specified, were used as received. Chemical analyses were carried out by the microanalytical laboratory of the School of Chemical Sciences, University of Illinois.

Deuterated solvents were obtained from Stohler Isotope Chemicals and from Merck Sharp and Dohme. 4-(2-Aminoethyl)diethylenetriamine (also known as tris(2-aminoethyl)amine or tren) was purchased from Ames Laboratories and 2-pyridinecarboxaldehyde and 6-methyl-2-pyridinecarboxaldehyde from Aldrich.

**Isolation of Tren·3HCl.** The tetramine, tren, was isolated as the trihydrochloride salt, tren·3HCl, from the commercially available liquid form, tris(2-aminoethyl)amine (Ames Laboratories). The following procedure was found necessary to isolate tren·3HCl in a pure form since the commercially available amine also contains some triethylenetetramine impurity. To 50 ml of absolute ethanol, 25 ml of the liquid amine was added and the solution cooled to 0°. Slow addition of concentrated HCl (so as to maintain the temperature near 0°) resulted in the precipitation of the white solid, tren·3HCl. The product was collected in fractions after each 5-ml addition of HCl until ~40 g of the solid had been collected. Each crop was recrystallized from a minimum amount of boiling water by addition of ethanol and analyzed by microanalysis before use. *Anal.* Calcd for $C_6H_{21}N_4Cl_3$: C, 28.15; H, 8.28; N, 21.92. Found (typically): C, 28.32; H, 8.10, N, 21.85.

**[Fe(Py)$_3$tren](PF$_6$)$_2$ (compound I)** was prepared by suspending powdered tren·3HCl (0.512 g, 2 mmol) in 25 ml of methanol containing 2-pyridinecarboxyaldehyde (0.642 g, 6 mmol). Dropwise addition of $NaOCH_3$ (0.324 g, 6 mmol) dissolved in 10 ml of methanol resulted in a light yellow solution which was allowed to stir at room temperature for 15 min. Addition of solid crystals of $FeCl_2 \cdot 4H_2O$ (0.40 g, 2 mmol) gave a deep purple solution immediately. After stirring for 10 min, $KPF_6$ (0.15 g, 5 mmol) dissolved in 50 ml of methanol was added dropwise with filtration. Upon cooling overnight at 0°, purple crystals were obtained. The product was recrystallized from an acetone–ether mixture approximately 1:3 by volume, collected by filtration, washed with ether, and dried 24 hr over $P_2O_5$ under vacuum at room temperature, yield 0.6 g (40%). *Anal.* Calcd for $FeC_{24}H_{27}N_7P_2F_{12}$: C, 37.96; H, 3.58; N, 12.91; Fe, 7.35. Found: C, 38.17; H, 3.52; N, 12.86; Fe, 7.37.

**[Fe(6-MePy)(Py)$_2$tren](PF$_6$)$_2$ (compound II)** was prepared by suspending powdered tren·3HCl (0.512 g, 2 mmol) in 50 ml of methanol containing 0.108 g (2 mmol) of $NaOCH_3$. The solution was stirred at room temperature for 20 min then 6-methyl-2-pyridinecarboxaldehyde (0.242 g, 2 mmol) was added and the solution became light orange in color. Stirring was continued for another 15 min and then another portion of $NaOCH_3$ (0.216 g, 4 mmol) was added. After 15 more min of stirring, 2-pyridinecarboxaldehyde

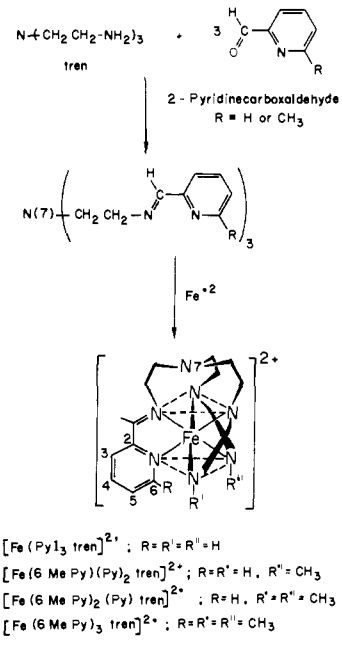


(I) $[Fe(Py)_3\,tren]^{2+}$ ; R = R' = R'' = H
(II) $[Fe(6\,Me\,Py)(Py)_2\,tren]^{2+}$ ; R = R' = H, R'' = $CH_3$
(III) $[Fe(6\,Me\,Py)_2(Py)\,tren]^{2+}$ ; R = H, R' = R'' = $CH_3$
(IV) $[Fe(6\,Me\,Py)_3\,tren]^{2+}$ ; R = R' = R'' = $CH_3$

**Figure 1.** Synthesis and structure of the Fe(II) cation complexes.

(0.428 g, 4 mmol) was added and the orange color of the solution darkened. Twenty milliliters of water was added in order to dissolve any remaining solid and the solution was allowed to stir at room temperature for another 20 min. Addition of $FeCl_2 \cdot 4H_2O$ (0.40 g, 2 mmol as a powdered crystalline solid) gave a deep purple solution. To this solution, a 20-ml aqueous solution containing $KPF_6$ (0.95 g, 5 mmol) was added dropwise with filtration. After cooling overnight at 0°, a reddish purple solid was obtained. The crystals were collected, purified, and dried as for I above. Yield is variable, 0.70 g (45%). *Anal.* Calcd for $FeC_{25}H_{29}N_7P_2F_{12}$: C, 38.82; H, 3.78; N, 12.68; Fe, 7.22. Found: C, 38.75; H, 3.75; N, 12.75; Fe, 7.19.

**[Fe(6-MePy)$_2$(Py)tren](PF$_6$)$_2$ (compound III)** was prepared by suspending powdered tren·3HCl (0.512 g, 2 mmol) in 50 ml of methanol containing 0.108 g (2 mmol) of $NaOCH_3$. The solution was stirred at room temperature for 20 min, then 2-pyridinecarboxaldehyde (0.214 g, 2 mmol) was added. Stirring was continued for another 15 min and then another portion of $NaOCH_3$ (0.216 g, 4 mmol) was added. After 15 more min of stirring 6-methyl-2-pyridinecarboxaldehyde (0.484 g, 4 mmol) was added. Twenty milliliters of water was added in order to dissolve any remaining solid and the solution was allowed to stir at room temperature for 20 minutes. Addition of $FeCl_2 \cdot 4H_2O$ (0.40 g, 2 mmol) and $KPF_6$ (0.95 g, 5 mmol) was carried out as for II above. After cooling overnight, purple crystals were collected, purified, and dried as for I above. Yield is variable 0.70 g (45%). *Anal.* Calcd for $FeC_{26}H_{31}N_7P_2F_{12}$: C, 39,66; H, 3.97; N, 12.45; Fe, 7.09. Found: C, 39.68; H, 3.96; N, 12.37; Fe, 6.97.

**[Fe(6-MePy)$_3$tren](PF$_6$)$_2$ (compound IV)** was prepared as above for I except that 6-methyl-2-pyridinecarboxyaldehyde (0.726 g, 6 mmol) was used in place of 2-pyridinecarboxaldehyde. Upon addition of the $FeCl_2 \cdot 4H_2O$, the solution became cherry red in color and the red solid, $[Fe(6\text{-}MePy)_3tren](PF_6)_2$, was isolated upon addition of $KPF_6$. After recrystallization and drying as for I above, the yield was 0.92 g (60%). *Anal.* Calcd for $FeC_{27}H_{33}N_7P_2F_{12}$: C, 40.44; H, 4.15; N, 12.24; Fe, 6.97. Found: C, 40.36; H, 4.29; N, 12.23; Fe, 6.98.

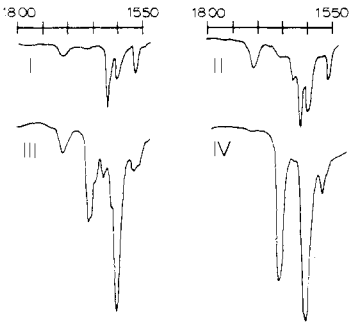


**Figure 2.** Infrared spectra of the Fe(II) hexafluorophosphate salts in the 1550–1800-cm$^{-1}$ region as Nujol mulls.

*Note:* For compounds II and III, where mixtures of products are possible, analytical results may not be sufficiently sensitive as a judge of compound purity. For samples with the analytical quality of those reported here, the Nujol mull infrared spectra in the 1550–1800-cm$^{-1}$ region (Figure 2) are moderately sensitive to the degree of methyl substitution and serve as a good diagnostic test for compound purity.

## Results and Discussion

**Magnetic Susceptibility Data and Molecular Structure Considerations.** In spin equilibrium complexes, both the high-spin and low-spin electronic states will be thermally populated. In octahedral (and pseudooctahedral) complexes of Fe(II), the available electronic states are $^1A_{1g}(t_{2g}^6)$ and $^5T_{2g}(t_{2g}^4e_g^2)$. Theoretical expressions for the temperature dependence of the magnetic susceptibility of such complexes have been reported in detail; additional splittings of the $^5T_{2g}$ state due to axial distortion, spin–orbit coupling, and Zeeman effects have also been considered.[4,5,7,21,22] In all of these cases, a Boltzman distribution over the lowest available states has been assumed, and additional terms due to higher energy electronic states have been shown to be small. In general, reported models for the temperature dependence of the magnetic susceptibility of octahedral Fe(II) complexes based on these assumptions have proven inadequate without the addition of extra parameters to the model. This observation, for samples studied only in the solid state, is not wholly unexpected since changes in the crystal structure of these complexes have been reported at low temperatures.[17,23] This might be interpreted in terms of a temperature dependent lattice effect were it not for the observation that the hydrotris(pyrazolyl)borate Fe(II) complex also exhibits an anomalous spin equilibrium in solution.[4] The failure of this system to conform to the simpler models has been discussed in some detail and available information suggests that a necessary addition to the models is one which assumes the added effect of either a temperature dependent crystal field[7,22,24] or a significant difference in the vibrational partition functions[21,25] of the two electronic states. It is worth noting here that for these two cases, variable temperature susceptibility expressions of the same form are generated and thus a least-squares fitting procedure, such as the one used here, will not be able to distinguish between them.

Complexes II, III and IV were extensively investigated in the solid state over the temperature range 80–470°K. The temperature dependency of I was not studied since its room temperature magnetic moment of 0.5 BM is typical of a low-spin pseudooctahedral Fe(II) complex. However, strongly temperature dependent magnetic moments were noted for the other three compounds in the solid state. In solution, only II and III were observed to exhibit this behavior over the range from 185 to 435°K. The results of these studies are presented graphically in Figures 3 and 4. Data appear in the microfilm edition.

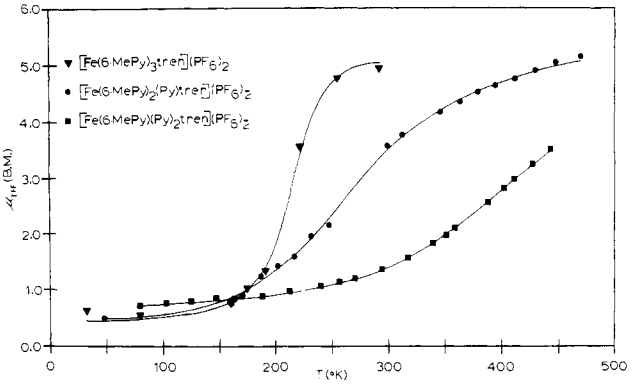


**Figure 3.** Solid state $\mu_{eff}$ in BM *vs.* temperature data for the Fe(II) complexes as $PF_6^-$ salts. The solid lines are best fit curves using the parameters in Table III.

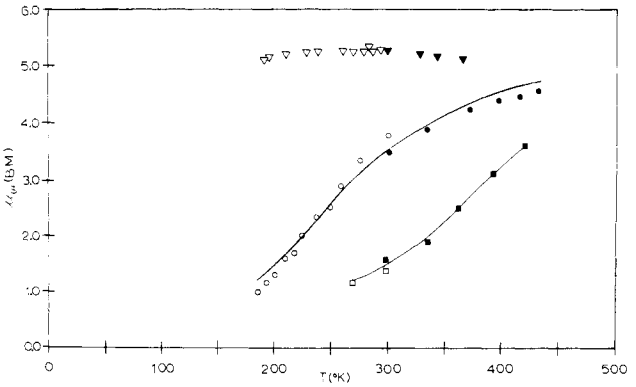


**Figure 4.** Solution state $\mu_{eff}$ in BM *vs.* temperature data for the Fe(II) complexes as $PF_6^-$ salts. The solid data points are for DMSO solutions and the open data points for acetone solutions. The solid lines are best fit curves using the parameters in Table III.

These results are consistent with the expected behavior for a high-spin ↔ low-spin equilibrium in an Fe(II) complex. Thermodynamic parameters for the dynamic equilibrium

$$Fe(II)(^1A_{1_g},\ ls) \rightleftharpoons Fe(II)(^5T_{2_g},\ hs)$$

may be readily evaluated using the following equations

$$m(hs) = (\chi_M - \chi_{ls})/(\chi_{hs} - \chi_{ls}) \quad (1)$$

$$m(ls) = (\chi_{hs} - \chi_M)/(\chi_{hs} - \chi_{ls}) \quad (2)$$

$$K_{eq} = m(hs)/m(ls) \quad (3)$$

where $\chi_M$ is the corrected molar susceptibility at a given temperature, $\chi_{hs}$ and $\chi_{ls}$ are the corrected molar susceptibilities of the pure high-spin and pure low-spin components, respectively, and $m$(hs) and $m$(ls) are the corresponding mole fractions. The pure high-spin behavior was evaluated from the data for IV in solution and the pure low-spin behavior was determined for each system, separately, from the low temperature data. Thermodynamic parameters have been evaluated from the equilibrium constants using ln $K$ *vs.* $1/T$ plots in the usual manner. In the solid state, these plots have a pronounced curvature at the low temperature end.

Only the linear portion of the plots was used in evaluating the parameters which appear in Table II. The curvature in these plots is probably due either to small inaccuracies in the values of $\chi_{ls}$ and $\chi_{hs}$ or results from a small amount of impurity. In either case, its effect is considered to be negligible.

The complexes discussed here are essentially octahedral in geometry with a superimposed trigonal distortion. We

Table II. Thermodynamic Parameters for the Spin Equilibria

| Compound ($PF_6^-$ salt) | | $\Delta H$ (kcal/mol)[a] | $\Delta S$ (eu)[a] | $T$ (°K)[b] |
|---|---|---|---|---|
| Solid | II | 4.79 (0.23) | 9.73 (0.61) | 294–472 |
| | III | 3.11 (0.23) | 9.68 (0.82) | 175–472 |
| | IV | 4.81 (1.86) | 20.85 (9.15) | 160–292 |
| Solution | II | 4.59 (3.27) | 9.98 (9.23) | 295–420 |
| | III | 2.84 (0.38) | 8.50 (1.51) | 184–433 |

[a] Thermodynamic parameters calculated from magnetic susceptibility data. Numbers in parentheses represent 99% confidence limits. [b] The temperature range over which the ln $K$ *vs.* $1/T$ plots are linear.

present here a theoretical expression for the temperature dependent magnetic susceptibility which is appropriate for such a system. Experience has shown that a good fit between experimental and calculated magnetic moments may be obtained using arbitrary values of certain parameters.[21,25] Thus, the quality of the fit is nearly independent of the spin-orbit coupling constant and the orbital reduction factor. In the derivation below, the orbital reduction factor is set equal to 1.0 throughout and spin-orbit coupling terms have not been included in the Hamiltonian for the system. The admittedly nonrealistic approximation that spin-orbit is zero does not invalidate any of the conclusions we shall draw, for the quality of the data fit is insensitive to any reasonable estmate of its magnitude.

The appropriate Hamiltonian for the splitting in the $^5T_{2g}$ state is given by eq 4. Here $\delta$ is the trigonal distortion pa-

$$\mathbf{H} = \delta(1 - \mathbf{L}_z'^2) + \beta\mathbf{H}(-\mathbf{L} + 2\mathbf{S}) \quad (4)$$

rameter. The isomorphism of the $^5P$ and $^5T$ states ($\mathbf{L}_z \rightarrow \mathbf{L}'_z$) has been exploited to evaluate the energies in terms of the $M_L$ quantum numbers. Evaluating the energies through second order in the Zeeman terms for the parallel and perpendicular cases yields the appropriate susceptibility expressions for the two orientations. The isotropic magnetic susceptibility is then calculated from eq 5. The resulting ex-

$$\chi = \frac{1}{3}\chi_{\parallel} + \frac{2}{3}\chi_{\perp} \quad (5)$$

pression for the magnetic susceptibility is given by eq 6

$$\chi = \frac{N\beta^2\left\{\left(\frac{250}{3kT} + \frac{20}{3\delta}\right)e^{-\Delta E/kT} + \left(\frac{40}{kT} - \frac{20}{3\delta}\right)e^{-(\Delta E+\delta)kT}\right\}}{1 + 5e^{-(\Delta E+\delta)/kT} + 10e^{-\Delta E/kT}} + N\alpha \quad (6)$$

where $\Delta E$ is the energy separation between the $^1A_1$ and the $^5E$ component of the octahedral $^5T_{2g}$ level, $\delta$ is the splitting of the $^5E$ and $^5A_1$ components of the $^5T_{2g}$ level and $N\alpha$ is the temperature independent paramagnetism. When $\delta$ is negative, $^5A_1$ is the lower of these two (see Figure 5).

The parameters $\Delta E$, $\delta$, and $N\alpha$ were evaluated by minimizing the sum of the squared deviations between the measured and calculated magnetic moments, $\Delta^2$ in eq 7. The ex-

$$\Delta^2 = \Sigma(\mu_{\text{exptl}} - \mu_{\text{calcd}})^2 \quad (7)$$

perimental data as in all previous cases were not reproduced by the resulting theoretical expression. It was found, however, that by replacing $\Delta E$ in eq 6, with the linear temperature function, eq 8, it was possible to reproduce the ob-

$$\Delta E = aT + b \quad (8)$$

served temperature dependence in the magnetic moments.[7] Table III contains the summary of the final parameters which best fit the experimental data as shown in Figure 3 and 4.

It should be pointed out that the more elaborate equations which may be used to reproduce susceptibility data for spin equilibrium systems do not provide any substantial advantage over the scheme used here. Spin-orbit coupling and orbital reduction factors cannot be fit by a least-squares scheme since $\Delta^2$ is simply too insensitive to changes in these two parameters. Thus, a set of reasonable values for these parameters must be assumed at the beginning of the fitting routine, and every different set will, in turn, yield different values for *a*, *b*, and $\delta$.

Table III. Parameter Fits for the Spin Equilibrium Systems

| Compound ($PF_6^-$ salt) | | $a$ | $b$ | $\delta$ | $N\alpha$ | $n$ | $10^3\Delta^2$ |
|---|---|---|---|---|---|---|---|
| Solid | II | −3.283 | 3115 | −1027 | 563 | 19 | 3 |
| | III | −3.343 | 2385 | −980 | 734 | 18 | 100 |
| | IV | −10.968 | 3939 | −1233 | 480 | 12 | 572 |
| Solution | II | −3.615 | 3120 | −1026 | 554 | 7 | 37 |
| | III | −2.317 | 2143 | −1040 | 700 | 17 | 533 |

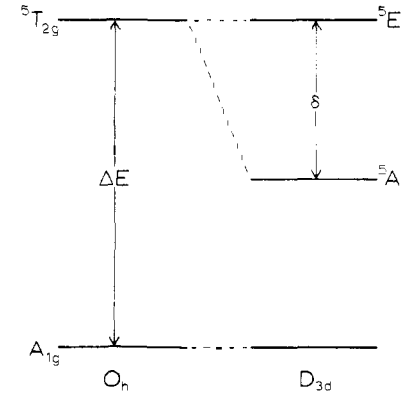


Figure 5. Energy levels for the $d^6$ configuration near to the $^5T_{2g} \rightarrow {}^1A_{1g}$ crossover.

In the series of complexes studied, two distinct types of anomolous magnetic behavior have been observed. The first, applicable to II and III, arises as a result of a nearly classical distribution over low lying spin states. The similarities between the magnetic moments obtained in the solid and solution for these two samples may be fortuitous but are more reasonably interpreted in terms of a similarly behaved spin equilibrium process in both environments. For III where magnetic data were taken in both acetone and DMSO, the slopes of the $\mu_{\text{eff}}$ *vs.* temperature plots differ as shown in Figure 4. The differing slopes for the two solvents may be due to some compound decomposition at the higher DMSO temperatures (see experimental section) or it may reflect a small, but legitimate, solvent dependency of the spin equilibrium process in solution. This possibility is under continuing investigation. A strikingly different sort of behavior is observed for IV. Here, the temperature dependence of the magnetic moments in solid and solution are completely different. The absence of a transition to the low-spin state in solution requires that some sort of *inter*molecular process be operative in the solid samples to produce the observed spin state change. The observation of a fairly sharp transition to the low-spin state at low temperatures is consistent with this conclusion and suggests that changes in the crystal lattice are influential in producing the transition observed in the solid for compound IV.

Two additional observations seem to confirm the suspicion that a phase change is taking place in the solid samples of IV at low temperature. The first is that the $BPh_4^-$ salt of IV has a magnetic moment of 4.3 BM at 86°K,[17] indicating that in this case a sharp transition to the low-spin state does not take place above this temperature, as it does for the $PF_6^-$ salt. It is presumed that lattice effects have been substantially altered by the anion change. Such anion dependency on spin equilibria in the solid state is not uncommon and has been reported, for example, for the tris(2-methyl-

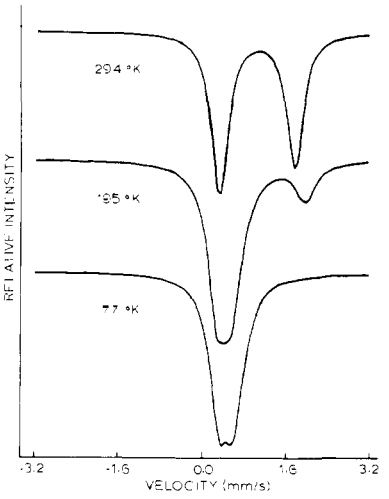


**Figure 6.** Simulated Mössbauer spectrum of $[Fe(6\text{-}MePy)_3tren](PF_6)_2$ relative to an iron foil standard.

1,10-phenanthroline)iron(II) cation.[14] Preliminary X-ray evidence[17] tends to confirm this conclusion even more strongly. These results, shown in Table I, show the expected relationship between the metal–nitrogen bond distance and spin state. The decrease in the Fe–N distances at low temperatures is accompanied by an ~4% decrease in the unit cell volume. This observation in conjunction with the results of the magnetic measurements on the $BPh_4^-$ salt of IV justify the conclusion that the driving force for the spin transition in solid samples of IV is a crystalline phase change and not *vice versa*. Spin equilibria of the type found only in the solid state, such as for the $PF_6^-$ salt of IV, should be differentiated from those of compounds II and III in that they are not wholly an electronic property of the isolated molecular complex. In fact, they may be considered to be "pseudo" spin equilibria in the sense that the lattice environment actually induces the property. In contrast, compounds II and III display similar magnetic behavior in both solution and solid, indicating that they represent examples of "true" spin equilibria where the property is essentially molecular in origin and reflects the electronic nature of the Fe(II) complex itself.

It is of interest to note that the X-ray measurements also provide information about the mechanism involved in "fine-tuning" the ligand field parameters into the region where the spin equilibrium may be observed. Calculations assuming Fe–N(pyridine) bond distances of 1.966 Å (as found in the X-ray structure of I)[16] reveal that the carbon atom of a pyridine ring 6-methyl substituent would be expected to lie above the plane of a second pyridine ring at a N(pyridine)–C(methyl) contact distance of ~2.4 Å.[15] This contact distance is well under the sum of the van der Waals radii for a nitrogen atom (1.5 Å) and a methyl group (2.0 Å). It is presumed that this steric interaction accounts for the increased Fe–N bond distances in IV relative to those of I which, in turn, reduces *Dq* sufficiently to give rise to a high-spin ground state at 300°K. For II and III, it is presumed that the intermediate degrees of methyl substitution produce "averaged" Fe–N bond lengths and ligand field splittings intermediate between the extremes quoted above for I and IV, thus giving rise to the observed magnetic behavior for the series. Clearly, then, the steric interactions systematically introduced by the step-wise methyl group substitution produces perturbations of the correct magnitude to permit a sensitive "fine-tuning" capability. It is anticipated that similar substituent effects (both steric and electronic) using multidentate ligands will be of general utility in the design and study of new spin equilibria systems. König and Watson have demonstrated that the mean differences in the Fe–N bond distances between high-spin and low-spin Fe(II) is expected to be about 0.12 Å.[23] For IV this value is apparently too conservative as an estimate since the average Fe–N bond length has already decreased by 0.12 Å in going from a high-spin state (5.0 BM) at 300°K to one of intermediate spin (2.3 BM) at 205°K. For total conversion of IV to a low-spin complex at around 150°K, it is not unreasonable to suppose that the overall difference in the Fe–N bond distances will increase beyond this value. X-Ray studies of IV at these low temperatures[17] as well as of II and III at room temperature[26] are presently in progress.

Table IV. Mössbauer Data for the $PF_6^-$ Salts

| Compound | $T$ (°K)[a] | Isomer shift[b] (mm/sec) | $\Delta E_Q$, quadrupole splitting (mm/sec) |
|---|---|---|---|
| I | 77 (ls) | 0.33 | 0.34 |
| | 293 (ls) | 0.28 | 0.32 |
| II | 4.2 (ls) | 0.18 | 0.42 |
| | 300 (ls) | 0.16 | 0.44 |
| III | 4.2 (ls) | 0.14 | 0.52 |
| | 300 (ls) | 0.12 | 0.54 |
| | 300 (hs) | 0.84 | 2.12[c] |
| IV | 77 (ls) | 0.41 | 0.30 |
| | 195 (ls) | 0.41 | 0.30 |
| | 195 (hs) | 1.19 | 1.55[c] |
| | 294 (hs) | 0.98 | 1.43 |

[a] Spin state of the Fe(II) center indicated in parentheses as either low-spin (ls) or high-spin (hs). [b] Measured relative to midpoint of room temperature iron foil spectrum. [c] Only one-half of doublet is fully resolved, part of the hs spectrum lies under one of the ls peaks (see Figure 6).

**Mössbauer Spectra.** Mössbauer data, while not extensive for the series of compounds, provide a unique spectroscopic handle for observing the changes in the Fe(II) spin state associated with the $^5T_2 \rightleftarrows {}^1A_1$ equilibrium. Furthermore, they serve to verify the fact that the observed magnetic properties in the solid arise from a spin equilibrium phenomenon and not from some other mechanism, *e.g.*, metal–metal exchange interactions. The data for the $PF_6^-$ salts are summarized in Table IV and typical spectra for compound IV are presented in Figure 6. For the temperature range investigated, compounds I and II show Mössbauer spectra having isomer shift values and quadrupole splittings ($\Delta E_Q$) characteristic of low-spin Fe(II) with $^1A_1$ ground states. This is in good qualitative agreement with the magnetic susceptibility data for the two compounds where $\mu_{eff}$ at room temperature is ~0.50 and ~1.50 BM, respectively. Apparently an ~5% population of the high-spin form for II at room temperature is not sufficient to resolve any high-spin Mössbauer signal from the spectrum background.

As usual for low-spin Fe(II), the spectra of I and II are relatively temperature independent. On the other hand, the Mössbauer spectra of III and IV reflect a strong temperature dependency. This dependency is most dramatically displayed by IV and is shown schematically in Figure 6 at 77, 195, and 294°K. With isomer shift and quadrupole splitting values of 0.41 and 0.30 mm/sec, the 77°K spectrum closely resembles that of other low-spin Fe(II) complexes. Again, this result is consistent with the experimentally determined magnetic moment of ~0.50 BM at 77°K. However, at 294°K, the large values for the isomer shift and quadrupole splitting are characteristic of high-spin Fe(II) complexes with a $^5T_2$ ground state where $\mu_{eff} \simeq 5.0$ BM. The 195°K spectrum shows features characteristic of both the high- and low-spin forms ($\mu_{eff} \simeq 2.0$ BM) with the relative intensities of the high- and low-spin resonances changing in the predicted fashion as the temperature is varied. The spectrum of III displays a similar temperature dependency, but

with a larger fraction of the low-spin form being populated for any given temperature. As indicated above by the magnetic studies, these temperature dependent Mössbauer results for III and IV are consistent with the presence of a $^5T_2 \rightleftarrows {}^1A_1$ spin equilibrium in the solid state for the two compounds. The fact that both high-spin and low-spin resonances are observed in these spectra demonstrates that *in the solid state* the lifetimes of the $^5T_2$ and $^1A_1$ states over the temperature range investigated are long-lived relative to the Mössbauer time scale, *i.e.*, $\gtrsim 10^{-7}$ sec. The same result has also been found for all other known Fe(II) $^5T_2 \rightleftarrows {}^1A_1$ spin equilibria where Mössbauer spectroscopy has been employed: $[Fe(phen)_2(NCS)_2]$,[5] $[Fe(phen)_2(NCSe)_2]$,[5] $[Fe(bipy)_2(NCS)_2]$,[27] the tris(2-aminomethylpyridine)iron(II) halides,[28] the 2-(2′-pyridyl)imidazoleiron(II) complexes,[6,29] and the poly(1-pyrazolyl)borate iron(II) system.[24] Of these examples, only the poly(1-pyrazolyl)borate iron(II) complex has also been characterized and studied *in the solution state*[30] and for this case it was observed that the spin lifetimes in solution are $\lesssim 10^{-7}$ sec for both high-spin and low-spin species.

**Proton Magnetic Resonance Spectra.** The pmr spectra obtained for complexes I–IV are all in qualitative agreement with the results obtained from the solution magnetic data. The diamagnetic compound I dissolved in acetonitrile-$d_3$ gives a spectrum consistent with its molecular structure as found in the solid state (Figure 1 and Table I). Downfield from internal TMS the methylene resonances appear as a complicated pattern centered at 3.4 ppm. The pyridine proton pattern, centered at 7.65 ppm, is also complicated but has been completely analyzed in terms of the four pyridine ring proton chemical shifts and coupling constants.[15] The methine proton resonance appears as a sharp singlet at 9.25 ppm.

The room temperature spectra of complexes II–IV are more difficult to interpret due to the proton isotropic shifts arising from the paramagnetism. The spectra are complicated, with a large number of resonances, and their detailed assignment has not been attempted here. For complex IV in acetone, nine distinct resonances (one for each of the chemically nonequivalent protons of the chelated $(6\text{-MePy})_3$tren ligand) are resolved with the isotropic shifts ranging from about 10 ppm upfield to 220 ppm downfield of TMS at 30°. These peaks all exhibit typical Curie law behavior as measured down to −60°. For II and III, the temperature dependences of the individual resonances are quite different from those observed for IV. The spectra of II and III as their $PF_6^-$ salts dissolved in acetone-$d_6$ are shown in Figure 7 relative to internal TMS. Individual resonances are difficult to follow as a function of temperature as they cross one another in a complicated fashion. It is clear from the spectra, however, that Curie type behavior is not exhibited by either complex since the spectrum tends to collapse into the diamagnetic region at low temperatures. In fact, at −39°, the pattern and integrated intensities of the 220-MHz spectrum of II agree well with that anticipated for the diamagnetic low-spin form, even though the complex is still somewhat paramagnetic ($\mu_{eff} \simeq 1.0$ BM). Assuming the proton assignments of methyl (1.5 ppm), methylene (3.5 ppm), pyridine (8 ppm), and methine (9.7 ppm), the observed integration areas are in the ratios 2.3:12.1:11.0:2.3 as compared to predicted ratios of 3:12:11:3. This agreement between the experimental and predicted integrated intensities offers the best evidence presently available that compound II is a single, discrete species in solution. Unfortunately, the spectrum of III, also shown in Figure 7, is still too broad and shifted at −42° ($\mu_{eff} \simeq 2.0$ BM) to obtain a good integration, although qualitatively it agrees well with the proposed structure for the complex.

The pmr data for II and III appear to be consistent with a rapid spin equilibrium giving rise to mole fraction weighted average resonance positions. Assuming that exchange is in the fast exchange temperature region, the appropriate expression for the spin state lifetime, $\tau$, is $\tau \ll 1/[2\pi(\delta\omega)]$ where $\delta\omega$ is the frequency separation, in hertz, between the two exchanging sites in the absence of exchange. Assuming shifts on the order of 200 ppm at 220 MHz for the high-spin species, as was observed for IV, and shifts of less than 10 ppm for the low-spin species, the upper limit for $\tau$ is $3.6 \times 10^{-6}$ sec. The recently measured spin lifetime for the bis(hydrotris(pyrazolyl)borate) iron(II) complex in solution is $3.2 \times 10^{-8}$ sec.[30] This value obtained by Beattie, *et al.*, using a laser T-jump technique, is certainly consistent with the pmr results obtained for the new spin equilibrium complexes reported here. Solution state thermodynamic parameters for II and III, as evaluated from the magnetic data, are similar to those for the bis(hydrotris(pyrazolyl)-borate) iron(II) complex with $\Delta H$ for the three species being 4.6, 2.8, and 3.9 kcal/mol, respectively. Thus, based on available data, $\tau$ values for II and III in solution are expected to be on the order of $10^{-7}$ to $10^{-8}$ sec in solution. Preparations are currently underway to measure $\tau$ directly and check this estimate.

**Electrochemical Data.** The Fe(II) → Fe(III) half-wave oxidation potentials for complexes I–IV were measured in an attempt to gain additional insight into electronic differences between the high-spin, low-spin, and spin-equilibrium Fe(II) complexes in solution. The polarographic data for the compounds are given in Table V. The half-wave potentials were obtained as the intercepts of the linear plots of the measured potential, $E$, *vs.* $\log [i/(i_d - i)]$. The data in Table V were collected in acetone solutions with 0.1 $M$ tetraethylammonium perchlorate electrolyte, using a rotating platinum electrode. The $E_{1/2}$ values are referenced to the sce and the limiting currents are all consistent with one electron ($n$ values) oxidations. It is well known that many species are characterized by irreversibility when studied at solid electrodes of the type used in this study.[31] That is apparently the case for these complexes as indicated by the slope of the $E$ *vs.* $\log [i/(i_d - i)]$ plots. For a strictly reversible one-electron oxidation, the slope would be 0.059. From inspection of the results in Table V, it is clear that the oxidations can, at best, be described as only quasi-reversible.

It will be noted that the $E_{1/2}$ values in Table V increase in a nonlinear monotonic fashion with the number of pyridine ring methyl groups. It was of interest to know whether this observed pattern for the Fe(II) → Fe(III) oxidations was due mainly to a change in the Fe(II) spin state or simply to an electronic effect of substituting methyl groups for protons on the pyridine rings. In order to help answer this question, two new low-spin pseudooctahedral Fe(II) complexes were prepared and their half-wave oxidation potentials determined. The complexes of interest were those derived from the condensation of 1 mol of triethylenetetramine (trien) and 2 mol of either 2-pyridinecarboxaldehyde (to

Table V. Fe(II) → Fe(III) Oxidation Potentials for the $PF_6^-$ Salts in Solution[a]

| Compound | $E_{1/2}$,[b,c] V | $n$ | Slope[c] of $E$ *vs.* $\log [i/(i - i_d)]$ |
|---|---|---|---|
| I | 0.917 (0.002) | 1 | 0.073 (0.003) |
| II | 0.948 (0.001) | 1 | 0.081 (0.002) |
| III | 0.989 (0.004) | 1 | 0.090 (0.006) |
| IV | 1.117 (0.008) | 1 | 0.074 (0.014) |

[a] Room temperature acetone solutions, $1 \times 10^{-3}$ $M$ in complex and 0.1 $M$ in $(Et_4N)ClO_4$. [b] Obtained at a spinning platinum electrode and referenced to the sce. [c] Numbers in parentheses represent 99% confidence limits.

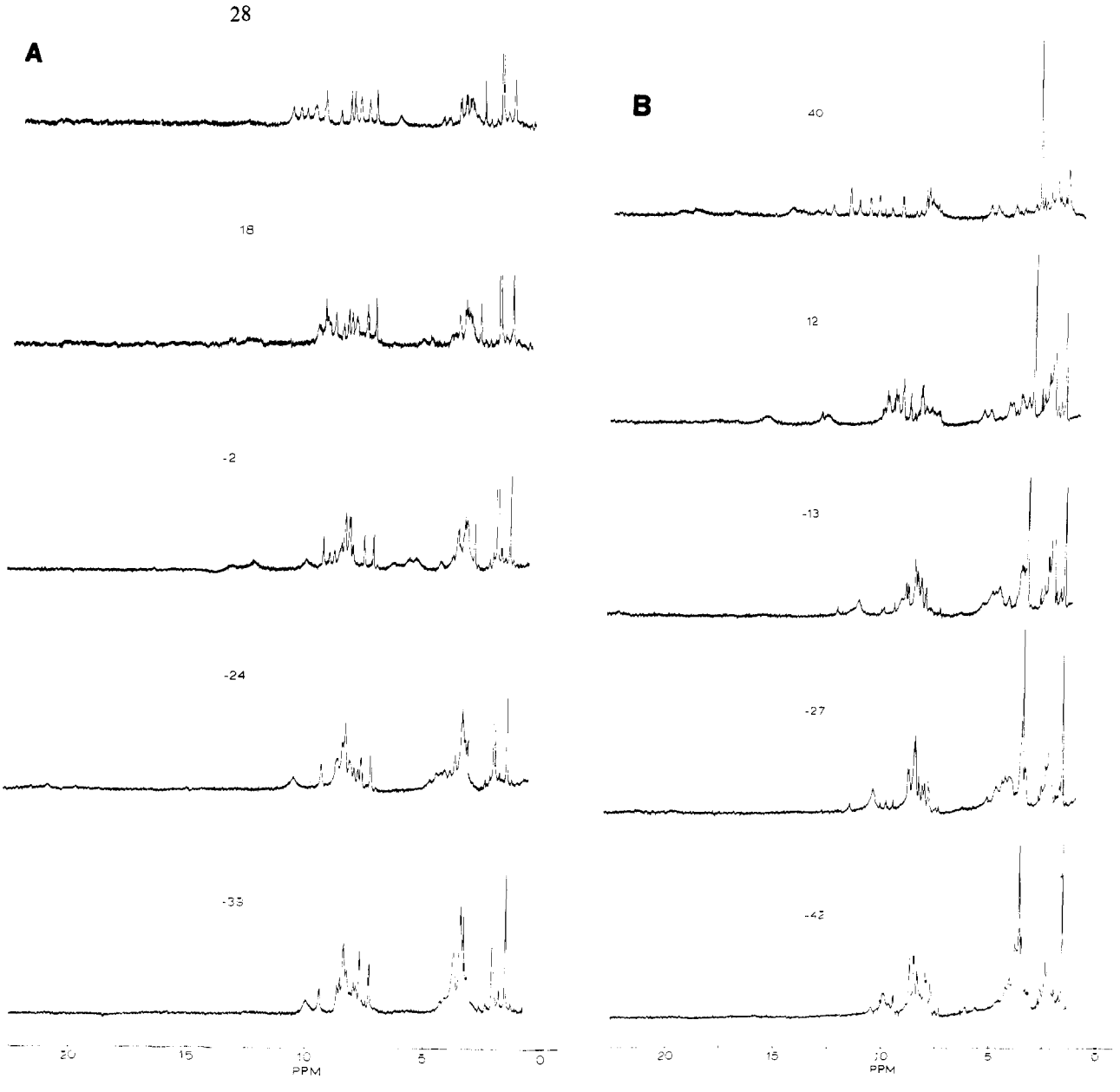


**Figure 7.** The 220-MHz pmr spectra of II (A) and III (B) as $PF_6^-$ salts in acetone-$d_6$. Reference is internal TMS.

yield $[Fe(Py_2trien)]^{2+}$) or 6-methyl-2-pyridinecarboxaldehyde (to yield $[Fe(6\text{-}MePy_2trien)]^{2+}$). Both complexes were isolated as their $PF_6^-$ salts and characterized as low-spin, pseudooctahedral Fe(II) species by their elemental analyses, solution conductivities (2:1 electrolytes in acetone), and proton magnetic resonance spectra. Inspection of molecular models indicated that the pyridine ring methyl groups for $[Fe(6\text{-}MePy_2trien)]^{2+}$ produce no *intra*molecular nonbonding interaction similar to those found in compounds II–IV and therefore it is not surprising that both $[Fe(Py_2trien)]^{2+}$ and $[Fe(6\text{-}MePy_2trien)]^{2+}$ are low-spin species. The $E_{1/2}$ values (determined under the conditions in Table V) for the two complexes were found to be 0.80 and 0.82 V for $[Fe(6\text{-}MePy_2trien)]^{2+}$ and $[Fe(Py_2trien)]^{2+}$, respectively. It is clear, therefore, that substitution of two methyl groups for two protons in the 6-position for these low-spin complexes results in a *decrease* of 0.02 V in the oxidation potential of the Fe(II) center. This methyl group dependence of the oxidation potential is the reverse of that found for compounds I–IV and therefore strongly indicates that the observed $E_{1/2}$ potentials in Table V are spin state dependent with the low-spin, high-spin, and intermediate-spin (equilibrium) Fe(II) centers displaying different oxidation potentials.

**Acknowledgment.** The authors wish to acknowledge the partial support of this research by the National Science Foundation through US NSF GP 31431X and by the National Institute of Health through its postdoctoral fellowship to L.J.W. We are grateful to Professor E. Münck for his help in obtaining some of the Mössbauer data and to Professor G. Stucky for providing information on the crystal structure of IV prior to publication. Technical assistance and valuable discussions during various stages of the endeavor by Mr. Robert Richman and Dr. Nicholas Kildahl are gratefully acknowledged.

**Supplementary Material Available.** A listing of magnetic susceptibility data will appear following these pages in the microfilm edition of this volume of the journal. Photocopies of the supplementary material from this paper only or microfiche (105 × 148 mm, 24× reduction, negatives) containing all of the supplementary material for the papers in this issue may be obtained from the Jour-

nals Department, American Chemical Society, 1155 16th St., N.W., Washington, D.C. 20036. Remit check or money order for $3.00 for photocopy or $2.00 for microfiche, referring to code number JACS-75-1722.

## References and Notes


(1) Presented in part at the 167th National Meeting of the American Chemical Society, Los Angeles, Calif., April 1974, INORG. 80.
(2) University of Illinois.
(3) William Marsh Rice University.
(4) J. P. Jesson, S. Trofimenko, and D. R. Eaton, *J. Amer. Chem. Soc.*, **89**, 3158 (1967).
(5) (a) E. König and K. Madeja, *Inorg. Chem.*, **6**, 48 (1967). (b) P. B. Merrithew and P. G. Rasmussen, *ibid.*, 325 (1972).
(6) (a) D. M. L. Goodgame and A. A. S. C. Machado, *Inorg. Chem.*, **8**, 2031 (1969). (b) A. H. Ewald, R. L. Martin, E. Sinn, and A. H. White, *ibid.*, **8**, 1837 (1969).
(7) E. König and S. Kremer, *Theor. Chim. Acta*, **20**, 143 (1971); **23**, 12 (1971).
(8) C. M. Harris, S. Kokot, H. R. H. Patil, E. Sinn, and H. Wong, *Aust. J. Chem.*, **25**, 1631 (1972).
(9) A. J. Cunningham, J. E. Fergusson, and H. K. L. Powell, *J. Chem. Soc., Dalton Trans.*, 2155 (1972).
(10) R. L. Martin and A. H. White, "Transition Metal Chemistry," Vol. 4, R. L. Carlin, Ed., 1968, p 113.
(11) E. K. Barefield, D. H. Busch, and S. M. Nelson, *Quart. Rev., Chem. Soc.*, **22**, 457 (1968).
(12) (a) H. Taube, "Electron Transfer Reactions of Complex Ions in Solution," Academic Press, New York, N.Y., 1970. (b) M. C. Palazzotto and L. H. Pignolet, *Inorg. Chem.*, **13**, 1781 (1974).
(13) M. Sharrock, E. Münck, P. G. Debrunner, V. Marshall, J. D. Lipscomb, I. C. Gunsalus, *Biochemistry*, **12**, 258 (1973).
(14) H. A. Goodwin and R. N. Sylva, *Aust. J. Chem.*, **21**, 83 (1968).
(15) Ph.D. Dissertation, L. J. Wilson, University of Washington, Seattle, 1971.
(16) C. Mealli and E. C. Lingafelter, *Chem. Commun.*, 885 (1970).
(17) G. Delker and G. D. Stucky, private communication.
(18) R. Kirchner and E. C. Lingafelter, private communication.
(19) D. F. Evans, *J. Chem. Soc.*, 2003 (1959).
(20) D. Ostfeld and I. A. Cohen, *J. Chem. Educ.*, **49**, 829 (1972).
(21) (a) E. König and A. S. Chakravorty, *Theor. Chim. Acta*, **9**, 151 (1967). (b) M. Soral and S. Seki, *J. Phys. Chem. Solids*, **35**, 555 (1974).
(22) E. König and S. Kremer, *Theor. Chim. Acta*, **22**, 45 (1971).
(23) E. König and K. J. Watson, *Chem. Phys. Lett.*, **6**, 457 (1970).
(24) J. P. Jesson, J. F. Weiher, and S. Trofimenko, *J. Chem. Phys.*, **48**, 2058 (1968).
(25) C. M. Harris and E. Sinn, *Inorg. Chim. Acta*, **2**, 296 (1968).
(26) D. Cullen and L. J. Wilson, to be submitted for publication.
(27) E. König, K. Madeja, and K. J. Watson, *J. Amer. Chem. Soc.*, **90**, 1146 (1968).
(28) G. A. Renovitch and W. A. Baker, Jr., *J. Amer. Chem. Soc.*, **89**, 6377 (1967).
(29) R. J. Dosser, W. J. Eilbeck, A. E. Underhill, P. R. Edwards, and C. E. Johnson, *J. Chem. Soc. A*, 810 (1969).
(30) J. K. Beattie, N. Sutin, D. H. Turner, and G. W. Flynn, *J. Amer. Chem. Soc.*, **95**, 2052 (1973).
(31) R. N. Adams, "Electrochemistry at Solid Electrodes," Marcel Dekker, New York, N.Y., 1969.


# On the Mechanism of Photochemical Decarbonylation of Acetyldicarbonyl-$\eta^5$-cyclopentadienyliron


**John J. Alexander**

*Contribution from the Department of Chemistry, University of Cincinnati, Cincinnati, Ohio 45221.*

*Received July 18, 1974*


**Abstract:** It is demonstrated that decarbonylation of $\eta^5$-$(C_5H_5)Fe(CO)_2{}^{13}C(O)CH_3$ either photochemically or in the mass spectrometer occurs with loss of a terminal carbonyl group. The intermediate resulting from the photochemical process undergoes nucleophilic attack by triphenylphosphine faster than methyl migration. Mass spectra of $\eta^5$-$(C_5H_5)Fe(CO)_2{}^{13}C(O)CH_3$ show differences in the fragmentation patterns which depend on the ionization energy. At 20 eV considerably more scrambling and loss of $^{13}CO$ is observed than at 70 eV.


Insertion and abstraction reactions involving metal-carbon bonds are well known in organometallic chemistry.[1] Carbon monoxide was one of the first small molecules found to give insertion products with metal alkyl complexes.[2]

$$CH_3Mn(CO)_5 + CO \underset{\Delta}{\rightleftharpoons} CH_3C(O)Mn(CO)_5 \qquad (1)$$

Two points are worthy of note in regard to reaction 1: first, that the reaction is thermally reversible to give the product resulting from CO abstraction out of the Mn-C bond; second, that the terms insertion and abstraction merely describe the structure of the product compared to that of the reactant. Indeed, it has been shown[3] that the "inserted" CO in reaction 1 is one of the CO's originally bonded to Mn.

Cyclopentadienyliron dicarbonyl alkyls and acyls will undergo reactions analogous to eq 1; however, much more vigorous conditions are required to effect these.[4,5]

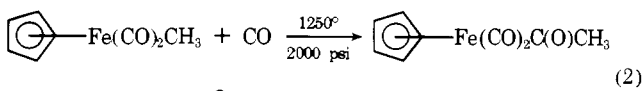


(2)

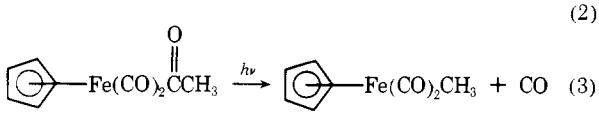


(3)

This fact has discouraged mechanistic studies on cyclopentadienyliron carbonylation reactions where the entering nucleophile is CO.

Our recent work on the chemical decarbonylation of organometallic acyl complexes[6] using chlorotris(triphenylphosphine)rhodium(I) led us to investigate the mechanism of decarbonylation of $\eta^5$-$(C_5H_5)Fe(CO)_2{}^{13}C(O)CH_3$ under photolytic conditions. The results of this investigation are reported here along with some information on fragmentation pathways of $\eta^5$-$(C_5H_5)Fe(CO)_2{}^{13}C(O)CH_3$ and $\eta^5$-$(C_5H_5)Fe(^{13}CO)(CO)CH_3$ in the mass spectrometer.

## Experimental Section

**Materials.** Solvents and chemicals were reagent grade and were used without further purification except for tetrahydrofuran which was distilled from calcium hydride. Chromatography was carried out on columns of acid-washed Grade I Woelm alumina. $\eta^5$-$(C_5H_5)Fe(CO)_2{}^{13}C(O)CH_3$ was prepared by a previously published procedure.[6] Purification was accomplished by repeated vacuum sublimation at 40° onto a Dry Ice-cooled probe. The compound exhibited terminal CO stretches at 2021 (s) and 1968 (s) $cm^{-1}$ in hexane. The acyl stretches occurred at 1671 (m) for $^{12}C{=}O$ and 1636 (m) $cm^{-1}$ for $^{13}C{=}O$.

**Decarbonylation of $\eta^5$-$(C_5H_5)Fe(CO)_2{}^{13}C(O)CH_3$.** The acetyl complex (0.50 g, 2.3 mmol) in 100 ml of hexane was irradiated under $N_2$ in a quartz vessel for 30 min with a Hanovia 450-W mercury vapor lamp. The solution was reduced in volume under a ni-